THE TRANSVERSE ENERGY AND THE CHARGED PARTICLE MULTIPLICITY IN A STATISTICAL MODEL WITH EXPANSION*

Dariusz Prorok

Institute of Theoretical Physics, University of Wrocław
Maksa Borna 9, 50-204 Wrocław, Poland

(Received October 4, 2004)

Global variables such as the transverse energy and the charged particle multiplicity and their ratio are evaluated, in a statistical model with expansion, for heavy-ion collisions from AGS to RHIC at $\sqrt{s_{NN}} = 200$ GeV. Full description of decays of hadron resonances is applied. The predictions of the model done at the freeze-out parameters established independently from observed particle yields and p_{T} spectra agree well with the experimental data. However, some (explicable) overestimation of the ratio has been found.

PACS numbers: 25.75.–q, 25.75.Dw, 24.10.Pa, 24.10.Jv

1. Introduction

The statistical model has been applied successfully in description of the soft part of particle production in heavy-ion collisions [1–14]. Namely, the particle yield ratios and p_{T} spectra were fitted accurately with the use of only four parameters (for particle ratio fits two parameters are enough: the temperature T and the baryon number chemical potential μ_B). Now, those parameters will be used to evaluate global observables: the transverse energy density $dE_{\mathrm{T}}/d\eta$, the charged particle multiplicity density $dN_{\mathrm{ch}}/d\eta$ and their ratio (for details see [15]). The advantage of such an approach is based on the fact that the transverse energy and charged particle multiplicity measurements are independent of hadron spectroscopy (in particular, no particle identification is necessary), therefore they could be used as an additional test of the self-consistency of a statistical model.

* Presented at the XLIV Cracow School of Theoretical Physics, Zakopane, Poland, May 28–June 6, 2004.

The experimentally measured transverse energy is defined as

$$E_{\mathrm{T}} = \sum_{i=1}^{L} \hat{E}_i \sin\theta_i \,, \tag{1}$$

where θ_i is the polar angle, $\hat{E}_i$ denotes $E_i - m_N$ (m_N means the nucleon mass) for baryons and the total energy E_i for all other particles, and the sum is taken over all L emitted particles [16]. Additionally, in the case of RHIC at $\sqrt{s_{NN}} = 200$ GeV, $E_i + m_N$ is taken instead of E_i for antibaryons [17].

The statistical model with single freeze-out is used (for details see [12]). The model very well reproduces ratios and p_{T} spectra of particles measured at RHIC [8–10]. The main assumption of the model is the simultaneous occurrence of chemical and thermal freeze-outs, which means that the possible elastic interactions after the chemical freeze-out are neglected. The conditions for the freeze-out are expressed by values of two independent thermal parameters: T and μ_B. The strangeness chemical potential μ_S is determined from the requirement that the overall strangeness of the gas equals zero.

The actually detected (stable) particles have two sources: (a) a thermal gas and (b) secondaries produced by decays and sequential decays of primordial resonances. The distributions of particles from source (a) are given by a Bose–Einstein or a Fermi–Dirac distribution at the freeze-out point. The distributions of secondaries (source (b)) can be obtained from the elementary kinematics of a many-body decay or from the superposition of two or more such decays (for details see [12, 15]). In the following, all possible (2-, 3- and 4-body) decays with branching ratios not less than 1% are considered. Also almost all cascades (with the exclusion of a very few like 4- or 5-step ones such that they proceed via at least one 3- or 4-body decay) are taken into account. It should be stressed that all contributions from weak decays are included in the presented analysis.

2. The foundations of the single-freeze-out model

The foundations of the model are as follows: (a) the chemical and thermal freeze-outs take place simultaneously, (b) all confirmed resonances up to a mass of 2 GeV from the Particle Data Tables [18] are taken into account, (c) a freeze-out hypersurface is defined by the equation

$$\tau = \sqrt{t^2 - r_x^2 - r_y^2 - r_z^2} = \mathrm{const} \,, \tag{2}$$

(d) the four-velocity of an element of the freeze-out hypersurface is proportional to its coordinate

$$u^\mu = \frac{x^\mu}{\tau} = \frac{t}{\tau} \left(1, \frac{r_x}{t}, \frac{r_y}{t}, \frac{r_z}{t}\right) , \tag{3}$$

(e) the transverse size is restricted by the condition $r = \sqrt{r_x^2 + r_y^2} < \rho_{\max}$. In this way one has two additional parameters of the model, τ and $\rho_{\max}$, connected with the geometry of the freeze-out hypersurface.

The maximum transverse-flow parameter (or the surface velocity) is given by

$$\beta_\perp^{\max} = \frac{\rho_{\max}/\tau}{\sqrt{1 + (\rho_{\max}/\tau)^2}}\,. \tag{4}$$

The invariant distribution of the measured particles of species i has the form [9, 10]

$$\frac{dN_i}{d^2p_{\rm T}\,dy} = \int p^\mu d\sigma_\mu\; f_i(p\cdot u)\,, \tag{5}$$

where $d\sigma_\mu$ is the normal vector on a freeze-out hypersurface, $p\cdot u = p^\mu u_\mu$, u_μ is the four-velocity of a fluid element and f_i is the final momentum distribution of the particle in question. The final distribution means here that f_i is the sum of primordial and simple and sequential decay contributions to the particle distribution (for details see [12]).

The pseudorapidity density of particle species i is given by

$$\frac{dN_i}{d\eta} = \int d^2p_{\rm T}\,\frac{dy}{d\eta}\,\frac{dN_i}{d^2p_{\rm T}\,dy} = \int d^2p_{\rm T}\,\frac{p}{E_i}\,\frac{dN_i}{d^2p_{\rm T}\,dy}\,. \tag{6}$$

Analogously, the transverse energy pseudorapidity density for the same species can be written as

$$\frac{dE_{{\rm T},i}}{d\eta} = \int d^2p_{\rm T}\,\hat{E}_i\cdot\frac{p_{\rm T}}{p}\,\frac{dy}{d\eta}\,\frac{dN_i}{d^2p_{\rm T}\,dy} = \int d^2p_{\rm T}\,p_{\rm T}\,\frac{\hat{E}_i}{E_i}\,\frac{dN_i}{d^2p_{\rm T}\,dy}\,. \tag{7}$$

For the quantities at midrapidity one has

$$\frac{dN_i}{d\eta}\Big|_{\rm mid} = \int d^2p_{\rm T}\,\frac{dN_i}{d^2p_{\rm T}\,dy}\,\frac{\sqrt{p_{\rm T}^2 + v_{\rm c.m.s}^2 m_i^2}}{m_{\rm T}}\,, \tag{8}$$

$$\frac{dE_{{\rm T},i}}{d\eta}\Big|_{\rm mid} = \begin{cases} \int d^2p_{\rm T}\;p_{\rm T}\;\frac{dN_i}{d^2p_{\rm T}\,dy}\;\frac{m_{\rm T}-\sqrt{1-v_{\rm c.m.s}^2}m_N}{m_{\rm T}}, i = \text{nucleon} \\ \int d^2p_{\rm T}\;p_{\rm T}\;\frac{dN_i}{d^2p_{\rm T}\,dy}, i \neq \text{nucleon}\,, \end{cases} \tag{9}$$

where $v_{\rm c.m.s}$ is the velocity of the center of mass of two colliding nuclei with respect to the laboratory frame (only for RHIC $v_{\rm c.m.s} = 0$). Note that for RHIC at $\sqrt{s_{NN}} = 200$ GeV there is the third possibility in Eq. (9): if $i =$ antinucleon, the analogous formula as for $i =$ nucleon but with $m_{\rm T} + m_N$ in the numerator holds.

The overall charged particle and transverse energy densities can be expressed as

$$\frac{dN_{\rm ch}}{d\eta}\Big|_{\rm mid} = \sum_{i\in B} \frac{dN_i}{d\eta}\Big|_{\rm mid}, \tag{10}$$

$$\frac{dE_{\rm T}}{d\eta}\Big|_{\rm mid} = \sum_{i\in A} \frac{dE_{{\rm T},i}}{d\eta}\Big|_{\rm mid}, \tag{11}$$

where A and B ($B \subset A$) denote sets of species of finally detected particles, namely the set of charged particles $B = \{\pi^+,\ \pi^-,\ K^+,\ K^-,\ p,\ \bar{p}\}$, whereas A also includes photons, $K^0_{\rm L}$, n and $\bar{n}$ [16].

3. Results

The general scheme reviewed in the previous section was formulated originally for RHIC [8–10] and then applied for SPS [14]. Here, this method will be used also for the AGS case. But the different model of the freeze-out hypersurface was applied for the description of $p_{\rm T}$ spectra there [1, 4]. In that model (for details see [19]), the freeze-out happens instantaneously in the r direction, *i.e.* at a constant value of t (*not* at a constant value of τ as here). The parameters connected with the expansion are the surface velocity $\beta_\perp^{\rm max}$ and $\rho_{\rm max}$. Therefore, the implementation of values of $\beta_\perp^{\rm max}$ obtained within that model into the presented one is entirely *ad hoc*, nevertheless it works surprisingly well. To put values of $\beta_\perp^{\rm max}$ from [1, 4] into formulae of Sect. 2, one should invert Eq. (4) to obtain

$$\frac{\rho_{\rm max}}{\tau} = \frac{\beta_\perp^{\rm max}}{\sqrt{1-(\beta_\perp^{\rm max})^2}}\,. \tag{12}$$

It should be recalled here that the value of τ itself is not necessary to calculate the transverse energy per charged particle, since this parameter cancels in the ratio.

The final results of numerical estimates of $dE_{\rm T}/d\eta|_{\rm mid}$ and $dN_{\rm ch}/d\eta|_{\rm mid}$ together with the corresponding experimental data are listed in Table I. To make predictions for the AGS case it has been assumed that the maximal transverse size $\rho_{\rm max}$ equals the average of radii of two colliding nuclei and the nucleus radius has been expressed as $R_A = r_0 A^{\frac{1}{3}}$, $r_0 = 1.12$ fm. Generally, the estimates agree well with the data. However, for RHIC the $11\% - 16\%$ underestimation of the charged particle density has been found. But this simply reflects the existing inconsistency in measurements of the charged particle multiplicity at RHIC. Namely, the sum of integrated charged hadron yields [20], after converting to $dN_{\rm ch}/d\eta$ [17], is substantially less then the directly measured $dN_{\rm ch}/d\eta|_{\rm mid}$ [21]. This is shown explicitly in the last column

of Table I. But values of the sum agree very well with the model predictions. Since the geometric parameters were established from the fits to the same p_{T} spectra, the agreement had to be obtained. Also for AGS the results agree qualitatively well with the data, in spite of the roughness of the method applied for this case. The overall error of evaluations of transverse energy and charged particle densities is about 0.5% and is caused by: (a) omission of the most complex cascades; (b) simplifications in numerical procedures for more involved cascades. The velocity of the center of mass of two colliding nuclei, $v_{\mathrm{c.m.s}}$, equals: 0 for RHIC, 0.994 for SPS Pb–Pb collisions at $158A$ GeV, 0.918 for AGS Au–Au collisions at $11A$ GeV and 0.678 for AGS Si–Pb collisions at $14.6A$ GeV.

TABLE I

Values of $dE_{\mathrm{T}}/d\eta|_{\mathrm{mid}}$ and $dN_{\mathrm{ch}}/d\eta|_{\mathrm{mid}}$ calculated in the framework of the statistical model with expansion. In the first column thermal and geometric parameters are listed for the corresponding collisions. In the third and last column experimental data for the most central collisions are given.

Collision case	$dE_{\mathrm{T}}/d\eta\|_{\mathrm{mid}}$ [GeV]		$dN_{\mathrm{ch}}/d\eta\|_{\mathrm{mid}}$	
	Theory	Experiment	Theory	Experiment
Au–Au at RHIC at $\sqrt{s_{NN}} = 200$ GeV: $T = 165.6$ MeV, $\mu_B = 28.5$ MeV $\rho_{\max} = 7.15$ fm, $\tau = 7.86$ fm ($\beta_\perp^{\max} = 0.67$) [11]	585 [a]	597 ± 34 [17]	589	699 ± 46 [17] 579 ± 29 [b] [22]
Au–Au at RHIC at $\sqrt{s_{NN}} = 130$ GeV: $T = 165$ MeV, $\mu_B = 41$ MeV $\rho_{\max} = 6.9$ fm, $\tau = 8.2$ fm ($\beta_\perp^{\max} = 0.64$) [12]	507	503 ± 25 [16]	555	622 ± 41 [21] 568 ± 47 [b] [20]
Pb–Pb at SPS: $T = 164$ MeV, $\mu_B = 234$ MeV $\rho_{\max} = 6.45$ fm, $\tau = 5.74$ fm ($\beta_\perp^{\max} = 0.75$) [13,14]	447	363 ± 91 [23]	476	464^{+20}_{-13} [23]
Au–Au at AGS: $T = 130$ MeV, $\mu_B = 540$ MeV $\beta_\perp^{\max} = 0.675$, $\rho_{\max} = 6.52$ fm [1,4]	224	≈ 200 [24]	271	≈ 270 [25]
Si–Pb at AGS: $T = 120$ MeV, $\mu_B = 540$ MeV $\beta_\perp^{\max} = 0.54$, $\rho_{\max} = 5.02$ fm [1,4]	57	≈ 62 [25]	91	$\approx 115 - 120$ [25]

[a] For the modified definition of E_{T}, *i.e.* $E_i + m_N$ is taken instead of E_i for antibaryons, see Eq. (1).

[b] For the charged particle multiplicity expressed as the sum of integrated charged hadron yields.

Values of the ratio $dE_{\rm T}/d\eta|_{\rm mid}/dN_{\rm ch}/d\eta|_{\rm mid}$ can be also calculated. They are collected in Table II, together with the corresponding data. The overall overestimation of the order of 15% has been obtained. In the RHIC case this is the result of the underestimation of $dN_{\rm ch}/d\eta|_{\rm mid}$, which has been explained earlier. But when in the denominator of the experimental ratio, $dN_{\rm ch}/d\eta|_{\rm mid}$ from the summing up of integrated hadron yields is put, the theoretical predictions agree very well with the data. Note that the similar inconsistency in charged particle measurements could have also been the origin of the discrepancy between model and experimental values of $dN_{\rm ch}/d\eta|_{\rm mid}$ seen in the AGS Si–Pb case. For SPS, the result agrees with the experimental value within errors. The overall error of model evaluations of the ratio is less than 1%.

TABLE II

Values of the ratio $dE_{\rm T}/d\eta|_{\rm mid}/dN_{\rm ch}/d\eta|_{\rm mid}$ calculated in the framework of the statistical model with expansion. In the last column experimental data for the most central collisions are given.

Collision case	$dE_{\rm T}/d\eta\|_{\rm mid}/dN_{\rm ch}/d\eta\|_{\rm mid}$ [GeV]	
	Theory	Experiment
Au–Au at RHIC at $\sqrt{s_{NN}} = 200$ GeV	0.99 [a]	0.87 ± 0.06 [17] 1.03 ± 0.08 [b]
Au–Au at RHIC at $\sqrt{s_{NN}} = 130$ GeV	0.91	0.81 ± 0.06 [16] 0.89 ± 0.09 [b]
Pb–Pb at SPS	0.94	0.78 ± 0.21 [23]
Au–Au at AGS	0.83	0.72 ± 0.08 [25]
Si–Pb at AGS	0.63	0.52-0.54 [25]

[a] For the modified definition of $E_{\rm T}$, *i.e.* $E_i + m_N$ is taken instead of E_i for antibaryons, see Eq. (1).
[b] Author calculations with the use of experimental values given in Table I and the denominator expressed as the sum of integrated charged hadron yields.

These results have been also depicted together with the data in Fig. 1. One can see that the relative positions of theoretical points agree very well with the data, they are shifted up only and this is the effect of the overestimation discussed earlier.

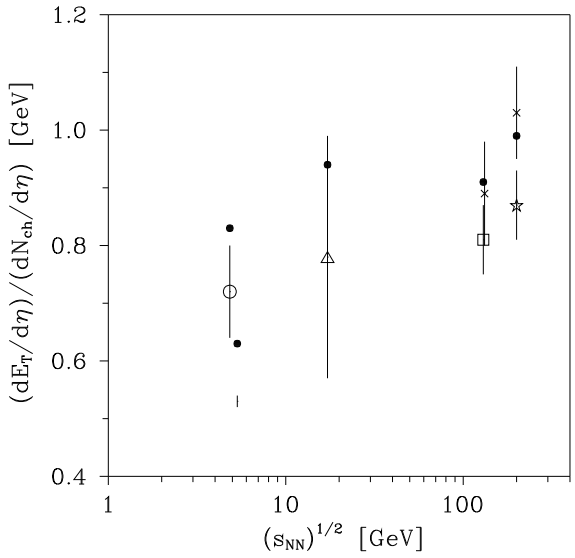

Fig. 1. Values of the transverse energy per charged particle at midrapidity for the most central collisions. Black dots denote evaluations of the ratio in the framework of the present model (the second column of Table II). Also data points for AGS [25] (a circle for Au–Au and a vertical bar for Si–Pb), SPS [23] (triangle), RHIC at $\sqrt{s_{NN}} = 130$ GeV [16] (square) and RHIC at $\sqrt{s_{NN}} = 200$ GeV [17] (star) are depicted. For RHIC, points with the sum of integrated charged hadron yields substituted for the denominator are also depicted (crosses).

4. Conclusions

The expanding thermal hadron gas model has been used to reproduce transverse energy and charged particle multiplicity pseudorapidity densities and their ratio measured at AGS, SPS and RHIC. The importance of the present analysis originates from the fact that the transverse energy and the charged particle multiplicity are *independent observables*, so they can be used as new tools to verify the consistency of predictions of a statistical model for all colliders simultaneously. The predictions have been made at the previous estimates of thermal and geometric freeze-out parameters obtained from analyses of measured particle ratios and $p_{\rm T}$ spectra at AGS [1, 4], SPS [13, 14] and RHIC [11, 12]. The overall good agreement, not only of the ratio but also absolute values of $dE_{\rm T}/d\eta\,|_{\rm mid}$ and $dN_{\rm ch}/d\eta|_{\rm mid}$, with the data has been achieved. And the observed discrepancies can be explained reasonably. This strongly supports the idea that the thermal expanding source is responsible for the soft part of the particle production in heavy-ion collisions. In addition, the description of various observables is consistent within one statistical model.

There are more arguments in favour of the above statement. One could think that this analysis is a kind of an internal consistency check of various measurements. And such a check could be done even in an model-independent way simply by integrating spectra of stable particles. But it can not be done without any external input. First, transverse momentum spectra are measured in *limited ranges*, so very important low-p_{T} regions are not covered by the data. Therefore, to obtain integrated yields some extrapolations below and above the measured ranges are used. In fact these extrapolations are only analytical fits without any physical reasoning, but contributions from regions covered by them account for 25%–40% of the yield [20]. On the other hand, a calorimeter acts very effectively in the low-p_{T} range, namely pions with $p_{\mathrm{T}} \leq 0.35$ GeV/c, kaons with $p_{\mathrm{T}} \leq 0.64$ GeV/c and protons and antiprotons with $p_{\mathrm{T}} \leq 0.94$ GeV/c are all captured [16]. Since the very accurate predictions for the transverse energy density at midrapidity have been obtained (see Table I), the present analysis can be understood as an indirect proof that in these unmeasurable p_{T} regions spectra are also explicable by means of the thermal source with flow and decays.

Moreover, it is impossible to check the consistency of the transverse energy data because not all stable hadron spectra are measured. This mainly concerns neutrons and K^0_{L}. Also it is impossible to extract hadron decay photons from the photon data. And again, the very good agreement of model estimates of the transverse energy density at midrapidity with the data can be interpreted as the strong argument that the production of neutral stable particles can be described in terms of the expanding thermal source with superimposed decays.

And as the last remark: in opposite to the transverse energy, there is some inconsistency (of the order of 10%) of the independent measurements of the charged particle multiplicity with the corresponding sums of integrated charged particle yields at RHIC (see Sect. 3). But at the present stage of investigation it is difficult to judge whether this inconsistency has the physical or experimental reason.

The author gratefully acknowledges very stimulating discussions with Wojciech Broniowski and Wojciech Florkowski. This work was supported in part by the Polish State Committee for Scientific Research (KBN) under Contract No. KBN 2 P03B 069 25.

REFERENCES

[1] P. Braun-Munzinger, J. Stachel, J.P. Wessels, N. Xu, *Phys. Lett.* **B344**, 43 (1995).

[2] P. Braun-Munzinger, J. Stachel, J.P. Wessels, N. Xu, *Phys. Lett.* **B365**, 1 (1996).

[3] J. Cleymans, D. Elliott, H. Satz, R.L. Thews, *Z. Phys.* **C74**, 319 (1997).

[4] J. Stachel, *Nucl. Phys.* **A610**, 509C (1996).

[5] P. Braun-Munzinger, I. Heppe, J. Stachel, *Phys. Lett.* **B465**, 15 (1999).

[6] F. Becattini, J. Cleymans, A. Keranen, E. Suhonen, K. Redlich, *Phys. Rev.* **C64**, 024901 (2001).

[7] P. Braun-Munzinger, D. Magestro, K. Redlich, J. Stachel, *Phys. Lett.* **B518**, 41 (2001).

[8] W. Florkowski, W. Broniowski, M. Michalec, *Acta Phys. Pol. B* **33**, 761 (2002).

[9] W. Broniowski, W. Florkowski, *Phys. Rev. Lett.* **87**, 272302 (2001).

[10] W. Broniowski, W. Florkowski, *Phys. Rev.* **C65**, 064905 (2002).

[11] A. Baran, W. Broniowski, W. Florkowski, *Acta Phys. Pol. B* **35**, 779 (2004).

[12] W. Broniowski, A. Baran, W. Florkowski, *Acta Phys. Pol. B* **33**, 4235 (2002).

[13] M. Michalec, Ph.D. thesis, `nucl-th/0112044`.

[14] W. Broniowski, W. Florkowski, *Acta Phys. Pol. B* **33**, 1935 (2002).

[15] D. Prorok, `hep-ph/0404209`, submitted to *Eur. Phys. J.* **A**.

[16] K. Adcox *et al.* [PHENIX Collaboration], *Phys. Rev. Lett.* **87**, 052301 (2001).

[17] A. Bazilevsky [PHENIX Collaboration], *Nucl. Phys.* **A715**, 486 (2003).

[18] K. Hagiwara *et al.* [Particle Data Group Collaboration], *Phys. Rev.* **D66**, 010001 (2002).

[19] E. Schnedermann, J. Sollfrank, U. Heinz, *Phys. Rev.* **C48**, 2462 (1993).

[20] K. Adcox *et al.* [PHENIX Collaboration], *Phys. Rev. Lett.* **88**, 242301 (2002).

[21] K. Adcox *et al.* [PHENIX Collaboration], *Phys. Rev. Lett.* **86**, 3500 (2001).

[22] S.S. Adler *et al.* [PHENIX Collaboration], *Phys. Rev.* **C69**, 034909 (2004).

[23] M.M. Aggarwal *et al.* [WA98 Collaboration], *Eur. Phys. J.* **C18**, 651 (2001).

[24] J. Barrette *et al.* [E814/E877 Collaboration], *Phys. Rev. Lett.* **70**, 2996 (1993).

[25] J. Barrette *et al.* [E877 Collaboration], *Phys. Rev.* **C51**, 3309 (1995).